DEPARTMENT OF THE INTERIOR
U.S. GEOLOGICAL SURVEY

In Situ Geomechanics of Crystalline and Sedimentary Rocks

Part IX: Prediction of Fault Slip in a Brittle Crust Under Multiaxial Loading Conditions

By

Bernard Amadei[1], William Z. Savage[2], and Henri S. Swolfs[2]

Open-File Report 87-503

1987

[1]University of Colorado
Boulder, CO 80309

[2]U.S. Geological Survey
Denver, CO 80225

CONTENTS

	Page
PREFACE	ii
ABSTRACT	1
INTRODUCTION	1
Basic Equations	2
Examples	7
SUMMARY	9
REFERENCES	11
APPENDIX	13

ILLUSTRATIONS

Figure 1. Geometry of the Problem: (a) Orientation angles of the fault and (b) state of stress across the fault..... 3

2. Regions (shaded) in which the normal to a fault plane must fall for slip to occur. Three-dimensional loading $\sigma_z \geq \sigma_y \geq \sigma_x > 0$. Figures are for $\tan\theta_j = 0.67$, $\sigma_1 = 10\sigma_3$ and σ_2/σ_3 1, 2, 3, 4, 5, 6, 8, and 10 in (a)···(h), respectively..... 8

3. Regions (shaded) in which the normal to a fault plane must fall for slip to take place. Three-dimensional state of stress σ_x, $\sigma_z = 0.1\sigma_x$ and $\sigma_y = -0.8\sigma_x$. The condition $F_n = 0$ is shown as a dashed line. Domain 1 is acceptable ($\sigma_n > 0$) when σ_x is positive. Domain 2 is acceptable ($\sigma_n > 0$) when σ_x is negative..... 10

IN SITU GEOMECHANICS OF CRYSTALLINE AND SEDIMENTARY ROCKS

PART IX: PREDICTION OF FAULT SLIP IN A BRITTLE CRUST UNDER MULTIAXIAL LOADING CONDITIONS

Bernard Amadei, William Z. Savage, and Henri S. Swolfs

PREFACE

This report is the ninth of a series summarizing the results of the U.S. Geological Survey's research program in geomechanics aimed at investigating and assessing the potential of crystalline and sedimentary rock masses as geological repositories of nuclear waste. The first eight parts of this series of reports are referenced below:

Savage, W.Z., and Swolfs, H.S., 1980, The long-term deformation and time-temperature correspondence of viscoelastic rock--an alternative theoretical approach, Pt. 1 of In situ geomechanics of crystalline and sedimentary rocks: U.S. Geological Survey Open-File Report 80-708, 21 p.

Smith, W.K., 1982, Two BASIC computer programs for the determination of in sity stresses using the CSIRO hollow inclusion stress cell and the USBM borehole deformation gage [Pt. 2 of In situ geomechanics of crystalline and sedimentary rocks]: U.S. Geological Survey Open-File Report 82-489, 40 p.

Swolfs, H.S., 1982, First experiences with the C.S.I.R.O. hollow-inclusion stress cell, Pt. 3 of In situ geomechanics of crystalline and sedimentary rocks: U.S.Geological Survey Open-File Report 82-990, 10 p.

Nichols, T.C., Jr., 1983, Continued field testing of the modified U.S. Geological Survey 3-D borehole stress probe, Pt. 4 of In situ geomechanics of crystalline and sedimentary rocks: U.S. Geological Survey Open-File Report 83-750, 11 p.

Savage, W.Z., Powers, P.S., and Swolfs, H.S., 1984, RVT--A FORTRAN program for an exact elastic solution for tectonic and gravity stresses in isolated symmetric ridges and alleys, Pt. 5 of In situ geomechanics of crystalline and sedimentary rocks: U.S. Geological Survey Open-File Report 84-827, 12 p.

Swolfs, H.S., and Powers, P.S., 1985, An update on two BASIC computer programs for the determination of in situ stresses using the CSIRO hollow inclusion cell and the USBM borehole deformation gage, Pt. 6 of In situ geomechanics of crystalline and sedimentary rocks: U.S. GeologicalSurvey Open-File Report 85-509, 15 p.

Savage, W.Z., and Swolfs, H.S., 1987, SLIP--A FORTRAN computer program for computing the potential for sliding on arbitrarily oriented weakness planes in triaxial stress states, Pt. 7 of In situ geomechanics of crystalline and sedimentary rocks: U.S. Geological Survey Open-File Report 87-82, 18 p.

Swolfs, H.S., and Nichols, T.C., Jr., 1987, Anisotropic characterization of Pierre Shale--Preliminary results, Pt. 8, of In situ geomechanics of crystalline and sedimentary rocks: U.S. Geological Survey Open-File Report 87-417, 9 p.

Published journal articles that report on the findings of this program are references below:

Swolfs, H.S., and Kibler, J.S., 1982, A note on the Goodman Jack: Rock Mechanics, v. 15, no. 2, p. 57-66.

Swolfs, H.S., 1983, Aspects of the size-strength relationship of unjointed rocks: Chapter 51 in Rock Mechanics--Theory-Experiment-Practice: 24th U.S. Symposium on Rock Mechanics, College Station, Texas, p. 501-510.

Swolfs, H.S., 1984, The triangular stress diagram - a graphical representation of crustal stress measurements: U.S. Geological Survey Professional Paper 1291, 19 p.

Swolfs, H.S., and Savage, W.Z., 1984, Site characterization studies of a volcanic cap rock, Chapter 39 in Rock Mechanics in Productivity and Protection: 25th U.S. Symposium on Rock Mechanics, Evanston, Illinois, p. 370-380.

Savage, W.Z., Swolfs, H.S., and Powers, P.S., 1985, Gravitational stresses in long symmetric ridges and valleys: International Journal of Rock Mechanics, Mining Sciences, and Geomechanical Abstracts, v. 22, no. 5, p. 291-302.

Swolfs, H.S., and Savage, W.Z., 1985, Topography, stresses, and stability at Yucca Mountain, Nevada, in Research & Engineering Applications in Rock Masses: 26th U.S. Symposium on Rock Mechanics, v. 2, p. 1121-1129.

Savage, W.Z., and Swolfs, H.S., 1986, Tectonic and gravitational stress in long symmetric ridges and valleys: Journal of Geophysical Research, v. 91, no. B3, p. 3677-3685.

Swolfs, H.S., and Savage, W.Z., 1986, Topographic modification of in situ stress in extensional and compressional tectonic environments: Proceedings of the International Symposium on Rock Stress and Rock Stress Measurements, Stockholm, Sweden, p. 89-98.

Swolfs, H.S., and Savage, W.Z., 1987, Analysis of slip potential in faulted rocks: Geological Society of America Abstracts with Programs, Rocky Mountain Section, v. 19, no. 5, p. 338.

Part XI: Prediction of Fault Slip in a Brittle Crust Under Multiaxial Loading Conditions

By

Bernard Amadei, William Z. Savage, and Henri S. Swolfs

ABSTRACT

Exact solutions are presented that describe the potential for slip reactivation on preexisting faults under a three-dimensional state of stress. Effects of fault cohesion and pore pressure are included in the general solutions to assess the extent of fault slip in crustal stress environments where one or several principal stress components may be tensile.

INTRODUCTION

The response of faulted rocks to three dimensional crustal loading depends largely on fault orientation and the anisotropy of the applied state of stress. Compared to intact rock, faulted rock is directional in its response to loading or unloading with reduced shear strength along the fault planes and vanishing or small tensile strength in a direction normal to the fault planes. These conclusions are based on laboratory triaxial and multiaxial tests on samples built up from blocks of model material (Brown, 1970; Ladanyi and Archambault, 1972; Einstein and Hirschfeld, 1973; Reik and Zacas, 1978). Three modes of failure of the test specimens were found; failure by sliding along faults, intact rock fracturing, or mixed sliding-intact rock fracturing. Fault sliding alone was found to take place only for faults favorably oriented with respect to the principal stresses.

Analytical models that describe the shear strength of an isotropic rock cut by a continuous single fault or a fault set have been proposed by Jaeger (1960) and Bray (1967). The intact rock and fault strength are described by Mohr-Coulomb criteria with different values of cohesion and friction. The models require the faulted rock response to depend only on the largest and smallest applied principal stresses σ_1, σ_3 without any contribution of the intermediate stress σ_2. These models are appropriate for slip reactivation under an axisymmetric state of stress σ_1, $\sigma_2 = \sigma_3$ or when the fault strikes parallel to the σ_2 direction with σ_2 not necessarily equal to σ_3.

The influence of the intermediate principal stress on fault slip has been analyzed graphically by Jaeger and Cook (1976) using a three-dimensional Mohr-circle construction. The results of the analysis were presented stereographically as regions in which the normal to a fault plane must fall for sliding on it to be possible. The stereographic projections were constructed for certain values of the stress ratios σ_2/σ_1 and σ_3/σ_1. More recently, an automated method has been developed by Savage and Swolfs (1986) to generate stereographic solutions numerically for stability analysis (Swolfs and Savage, 1987).

The three-dimensional analyses of Jaeger and Cook (1976) and Savage and Swolfs (1986) take σ_1, σ_2 and σ_3 to be compressive, thereby satisfying the physical constraint that the normal stress across the faults remains compressive. An exact solution is presented here for the bounding contours of the regions (in stereographic projection) in which the normal to a fault plane must fall for slip to be possible under a triaxial state of stress. The analysis allows any of the stress components σ_1, σ_2, σ_3 to be tensile. This is necessary because of the range of three-dimensional stress fields in rock masses resulting from loading or unloading and topography (Amadei et al., 1986; Savage et al., 1985; Savage and Swolfs, 1986). The different regions in the stereographic projection are obtained by combining the sterographic representations of the fault shear strength criterion and the positive normal stress condition. The influence of pore pressure on the extent of these regions is briefly discussed. A FORTRAN 77 program (Stereo 4.for) for the exact solutions is included in the Appendix. This program was used to generate the data for Figures 2 and 3.

Basic Equations

Consider a fault whose orientation with respect to a reference cartesian coordinate system xyz is shown in Figure 1a. Let x'y'z' be another coordinate system attached to the fault plane such that the x'-axis is along the upward normal and the y' and z' axes are in the fault plane. The z'-axis is in the xz plane and the y'-axis contains the dip direction. The orientation of the fault is defined by an azimuth angle β varying between 0 and 2π and a dip angle Ψ ranging between 0 and $\pi/2$. The upward unit vector $\vec{n}$ parallel to the x' axis has direction cosines $\bar{x}$, $\bar{y}$, $\bar{z}$ such that:

$$\begin{aligned} \bar{x} &= \sin\Psi \cos\beta \\ \bar{y} &= \cos\Psi \\ \bar{z} &= \sin\Psi \sin\beta \end{aligned} \tag{1}$$

Let σ_x, σ_y, σ_z be the principal stresses in the x, y, and z directions, respectively. Note that no ordering with respect to magnitude is implied; that is, σ_x, σ_y, and σ_z can have arbitrary values relative to each other. The state of stress across the fault can be defined by a stress vector with normal and shear components σ_n, τ (Figure 1b) such that:

$$\sigma_n = \sigma_x\bar{x}^2 + \sigma_y\bar{y}^2 + \sigma_z\bar{z}^2 \tag{2a}$$

$$\tau^2 = \sigma_x^2\bar{x}^2 + \sigma_y^2\bar{y}^2 + \sigma_z^2\bar{z}^2 - \sigma_n^2 \tag{2b}$$

The shear stress τ is also the resultant of the shear stress components $\tau_{x'y'}$ and $\tau_{x'z'}$ acting in the fault plane, that is,

$$\tau^2 = \tau^2_{x'y'} + \tau^2_{x'z'} \tag{3}$$

with, for the orientation shown in Figure 1a,

$$\begin{aligned} \tau_{x'y'} &= \sin\Psi \cos\Psi \, (\sigma_y - \sigma_x\cos^2\beta - \sigma_z\sin^2\beta) \\ \tau x'z' &= -\sin\beta \cos\beta \sin\psi \, (\sigma x - \sigma z) \end{aligned} \tag{4}$$

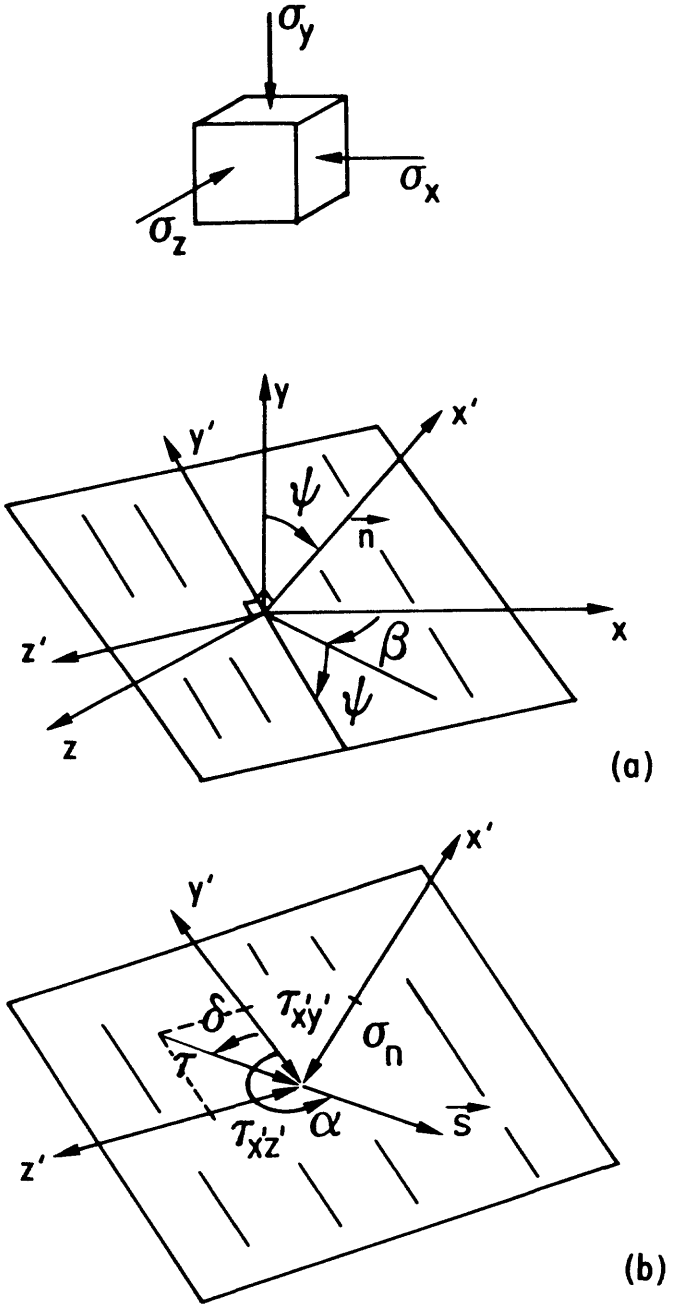

Fig. 1. Geometry of the Problem: (a) Orientation angles of the fault and (b) state of stress across the fault.

The orientation of the shear stress τ with respect to the y', z' axes is defined by the angle δ or,

$$\delta = \tan^{-1}\left(\frac{\tau_{x'z'}}{\tau_{x'y'}}\right) = \tan^{-1}\left(\frac{\sin\beta\cos\beta\,(\sigma_z-\sigma_x)}{\cos\psi\,(\sigma_y-\sigma_x\cos^2\beta-\sigma_z\sin^2\beta)}\right) \quad (5).$$

Note that the positive sign convention has been used for compressive stresses. The positive directions of the normal and shear stress components are shown in Figures 1a and 1b.

The shear strength of the fault is assumed to be defined by a Coulomb failure criterion with friction angle ϕ_j and zero cohesion; that is,

$$|\tau| = \sigma_n \tan\phi_j \quad (6)$$

Fault cohesion c_j and pore pressure p_w can be added to the analysis presented below by replacing σ_n by:

$$\sigma_n + \frac{c_j}{\tan\phi_j} - P_w \quad (7)$$

where $\sigma_n - P_w$ is the effective normal stress.

Equation (6) can also be expressed in terms of the principal stress components σ_x, σ_y, σ_z by squaring eq. (6) and by substituting eqs. (2a) and (2b) into (6). Let F_f be equal to $\tau^2 - \sigma_n^2\tan^2\phi_j$. Then, the fault slip criterion is such that:

$$\begin{aligned} F_f = {} & \sigma_x^2(\bar{x}^2 - \bar{x}^4(1+\tan^2\phi_j)) + \sigma_y^2(\bar{y}^2 - \bar{y}^4(1+\tan^2\phi_j)) \\ & + \sigma_z^2(\bar{z}^2 - \bar{z}^4(1+\tan^2\phi_j)) - 2\sigma_x\sigma_y\bar{x}^2\bar{y}^2(1+\tan^2\phi_j) \\ & - 2\sigma_x\sigma_z\bar{x}^2\bar{z}^2(1+\tan^2\phi_j) - 2\sigma_y\sigma_z\bar{y}^2\bar{z}^2(1+\tan^2\phi_j) = 0 \end{aligned} \quad (8)$$

For a plane with orientation angles β and ψ, the condition $F_f = 0$ corresponds to limiting equilibrium. No slip will take place if F_f is negative. Slip will occur if F_f is positive. The corresponding direction of slip can be defined by a unit vector $\vec{s}$ with coordinates (o, cosα, sinα) in the x'y'z' coordinate system as shown in Figure 1b. Using the value for the angle δ given in eq. (5), the angle α is equal to $\delta + \pi$ if $\tau_{x'y'}$ is positive and δ if $\tau_{x'y'}$ is negative. When $\tau_{x'y'}$ vanishes, α is equal to $3\pi/2$ if $\tau_{x'z'}$ is positive or $\pi/2$ if $\tau_{x'z'}$ is negative.

Unlike the Mohr-Coulomb criterion for intact rock which depends only on the major and minor principal stresses, the present fault-slip criterion depends on all three applied principal stresses. The fault is also assumed to have zero tensile strength implying that eq. (6) is only valid if the normal stress σ_n remains positive; that is, the following condition is satisfied

$$F_n = \sigma_x\bar{x}^2 + \sigma_y\bar{y}^2 + \sigma_z\bar{z}^2 > 0 \quad (9)$$

The functions F_f and F_n defined in eqs. (8) and (9) depend on the stress components σ_x, σ_y, σ_z and the fault upward normal coordinates $\bar{x}$, $\bar{y}$, and $\bar{z}$. These two functions can be used to find, for a given state of stress σ_x, σ_y, σ_z, the fault orientations for which slip is possible and the corresponding slip directions. The orientations can be represented by the $\bar{x},\bar{y},\bar{z}$ coordinates of the joint upward normal $\vec{n}$ or by the coordinates (x_o, z_o) of the stereographic projection of vector $\vec{n}$ on the xz plane following the method given by Goodman and Shi (1985). The coordinates x_o, z_o are related to $\bar{x}$, $\bar{y}$, $\bar{z}$ by:

$$x_o = \frac{R\bar{x}}{1+\bar{y}} \quad \text{and} \quad z_o = \frac{R\bar{z}}{1+\bar{y}} \tag{10}$$

where R is the radius of the reference sphere.

Substituting $\bar{y}^2 = 1-\bar{x}^2-\bar{z}^2$ into eq. (8) with $\sigma_y = m\sigma_x$ and $\sigma_z = n\sigma_x$ and assuming that σ_x does not vanish, the fault slip criterion can be expressed as follows:

$$\begin{aligned} F_f = {} & \sigma_x^2(-\bar{x}^4(1+\tan^2\phi_j)(m-1)^2 - \bar{z}^4(1+\tan^2\phi_j)(m-n)^2 \\ & + \bar{x}^2(m-1)(2m(1+\tan^2\phi_j) - 1 - m) \\ & + \bar{z}^2(m-n)(2m(1+\tan^2\phi_j) - m - n) \\ & + 2\bar{x}^2\bar{z}^2(1+\tan^2\phi_j)(m-n)(1-m) - m^2\tan^2\phi_j) = 0 \end{aligned} \tag{11}$$

Equation (10) gives the relationship that must exist between the stress ratios m and n and the $\bar{x},\bar{z}$ coordinates of the normal to a fault plane for slip to take place.

For given values of m and n, and the friction angle ϕ_j, eq. (10) can be used to find all the fault orientations for which the condition of limiting equilibrium (eq. (6)) is satisfied. The curve $F_f = 0$ separates the reference circle into two regions; a region where fault slip takes place for which $F_f > 0$ and a stable region for which $F_f < 0$. Note that for non-vanishing m and n value, the three principal planes always belong to the stable region.

Due to symmetry in both the x and z axes, the graph of $F_f = 0$ needs to be only constructed in the first quadrant of the stereographic projection. This can be done analytically by fixing $\bar{x}$ to an arbitrary value between 0 and 1 and rearranging eq. (10) as follows:

$$F_f = \sigma_x^2(a\bar{z}^4 + b\bar{z}^2 + c) = 0 \tag{12}$$

with

$$a = -(1+\tan^2\phi_j)(m-n)^2$$

$$b = (m-n)(2m(1+\tan^2\phi_j)-m-n) + 2\bar{x}^2(1+\tan^2\phi_j)(m-n)(1-m)$$

$$c = -\bar{x}^4(1+\tan^2\phi_j)(m-1)^2 + \bar{x}^2(m-1)(2m(1+\tan^2\phi_j)-1-m) - m^2\tan^2\phi_j$$

As long as a does not vanish (that is, m is not equal to n) eq. (11) has four roots $\bar{z}_1$, $\bar{z}_2$, $\bar{z}_3$, $\bar{z}_4$ such that:

$$\bar{z}_1 = \sqrt{\frac{-b + \sqrt{b^2 - 4ac}}{2a}} \quad ; \quad \bar{z}_2 = \sqrt{\frac{-b - \sqrt{b^2 - 4ac}}{2a}} \tag{13}$$

and $\bar{z}_3 = -\bar{z}_1$, $\bar{z}_4 = -\bar{z}_2$. A fault plane can be associated with each real and positive root $\bar{z}$, that is a solution of eq. (11), as long as $0 \leq \bar{y}^2 = 1-\bar{x}^2-\bar{z}^2 \leq 1$. The corresponding plane upward normal has components $\bar{x},\bar{z},\bar{y} = \sqrt{1-\bar{x}^2-\bar{z}^2}$ and its stereographic projection coordinates are given by eq. (10). The graph of $F_f = 0$ can be constructed by repeating the above procedure for a large number of values of $\bar{x}$.

If m is equal to n (that is, σ_y is equal to σ_z) the a and b coefficients in eq. (11) vanish and F_f reduces to $c\sigma_x^2$. The function F_f vanishes for four values of $\bar{x}$,

$$\bar{x}_1 = \sqrt{\frac{-b' + \sqrt{b'^2 - 4a'c'}}{2a}} \quad ; \quad \bar{x}_2 = \sqrt{\frac{-b' - \sqrt{b'^2 - 4a'c'}}{2a}} \tag{14}$$

and $\bar{x}_3 = -\bar{x}_1$, $\bar{x}_4 = -\bar{x}_2$ where,

$$a' = -(1 + \tan^2\phi_j)(m-1)^2$$

$$b' = (m-1)(2m(1 + \tan^2\phi_j)-1-m)$$

$$c' = -m^2\tan^2\phi_j$$

The roots exist as long as m and n are not equal to unity (hydrostatic state of stress) for which F_f is equal to $-\sigma_x^2\tan^2\phi_j$ and fault stability always takes place. For each real and positive root $\bar{x}$ solution of $F_f = 0$ that is less than or equal to unity, a fault plane can be associated with any arbitrary value of $\bar{z}$ such that $0 \leq \bar{y}^2 = 1-\bar{x}^2-\bar{z}^2 \leq 1$.
The corresponding plane upward normal has components $\bar{x},\bar{z},\bar{y} = \sqrt{1-\bar{x}^2-\bar{z}^2}$ and its stereographic projection coordinates are given by eq (10). The graph of $F_f = 0$ can be constructed by repeating the above procedure for a large number of values of $\bar{z}$.

The graph of $F_f = 0$ is further limited to the region of the stereographic projection for which the normal stress remains positive. Using the normality condition $\bar{y}^2 = 1-\bar{x}^2-\bar{z}^2$, the positive normal stress condition (eq. (9)) can be expressed as follows:

$$F_n = \sigma_x(\bar{x}^2(1 - m) + \bar{z}^2(n - m) + m) > 0 \tag{15}$$

The graph of $F_n = 0$ on the reference circle can be constructed with the same analytical procedure used for the graph of F_f. As long as m is not equal to n and for a fixed value of $\bar{x}$ ranging between 0 and 1, the condition $F_n = 0$ has two roots $\bar{z}$ and $-\bar{z}$ with:

$$\bar{z} = \sqrt{\frac{\bar{x}^2(m-1) - m}{(n-m)}} \tag{16}$$

If $\bar{z}$ is real and is such that $0 \leq \bar{y}^2 = 1-\bar{x}^2-\bar{z}^2 \leq 1$, the fault plane with upward normal coordinates $\bar{x},\bar{z},\bar{y} = \sqrt{1-\bar{x}^2-\bar{z}^2}$ belongs to the curve $F_n = 0$. The graph of $F_n = 0$ can be constructed by repeating the procedure for several values of $\bar{x}$.

If m is equal to n, $F_n = 0$ reduces to $\sigma_x(\bar{x}^2(1-m)+m) = 0$ which has two roots $\bar{x} = \sqrt{m/(m-1)}$ and $-\bar{x}$. If $\bar{x}$ is real, and less than or equal to unity, the graph of $F_n = 0$ can be constructed by choosing arbitrary values of $\bar{z}$ such that $0 \leq \bar{y}^2 = 1-\bar{x}^2-\bar{z}^2 \leq 1$.

In the expressions for the fault slip criterion (eq. (8)) and the positive normal stress condition (eq. (9)), it is assumed that the fault has no cohesion and is dry. As previously mentioned, these two equations can be modified to include fault cohesion c_j and water pressure P_w by substituting eq. (7) for the normal stress in eq. (6). For water pressure only, this substitution is equivalent to replacing σ_x, σ_y, and σ_z in eqs. (8) and (9) by the following effective stress components:

$$\sigma_x' = \sigma_x - P_w, \quad \sigma_y' = \sigma_y - P_w, \text{ and } \sigma_z' = \sigma_z - P_w.$$

If σ_x' does not vanish, the stress ratios m and n are now equal to σ_y'/σ_x' and σ_z'/σ_x', respectively.

The above substitution can be used to study for a given state of stress, $\sigma_x,\sigma_y,\sigma_z$, the influence of water pressure on the range of fault orientations for which slip can take place. Let $m_o = \sigma_y/\sigma_x$ and $n_o = \sigma_z/\sigma_x$ be the total stress ratios with σ_x not equal to zero. For a fixed value of P_w, the stress ratios m and n are now equal to:

$$m = \frac{m_o - p_w/\sigma_x}{1 - P_w/\sigma_x} \qquad n = \frac{n_o - P_w/\sigma_x}{1 - P_w/\sigma_x} \tag{17}$$

The graph of $F_f = 0$ and the region $F_n = \sigma_n' = \sigma_n - P_w > 0$ can be constructed for the values of m and n given in eq. (16) with the same analytical procedure used for the dry case.

Examples

The closed-form solution presented here gives the regions in stereographic projection in which the normal to a fault plane must fall for slip to occur under a three-dimensional state of stress and dry or wet conditions. Some illustrative examples are presented below. In all the examples, the slip regions are shown in a quadrant because of symmetry.

Figure 2, generated by using the closed-form solution, is identical to Figure 3.8.2 given by Jaeger and Cook (1976) which was obtained by using a three-dimensional Mohr circle construction and a friction coefficient $\tan\phi_j$ of 0.67. The stresses σ_z and σ_x are assumed to be positive and to be respectively the major and minor principal stresses σ_1,σ_3 with $\sigma_1 = 10\sigma_3$ (n=10). The intermediate stress $\sigma_y = \sigma_2$ (vertical) varies between σ_3 (m = 1) in Figure 2a and σ_1 (m = 10) in Figure 2h. Cases corresponding to

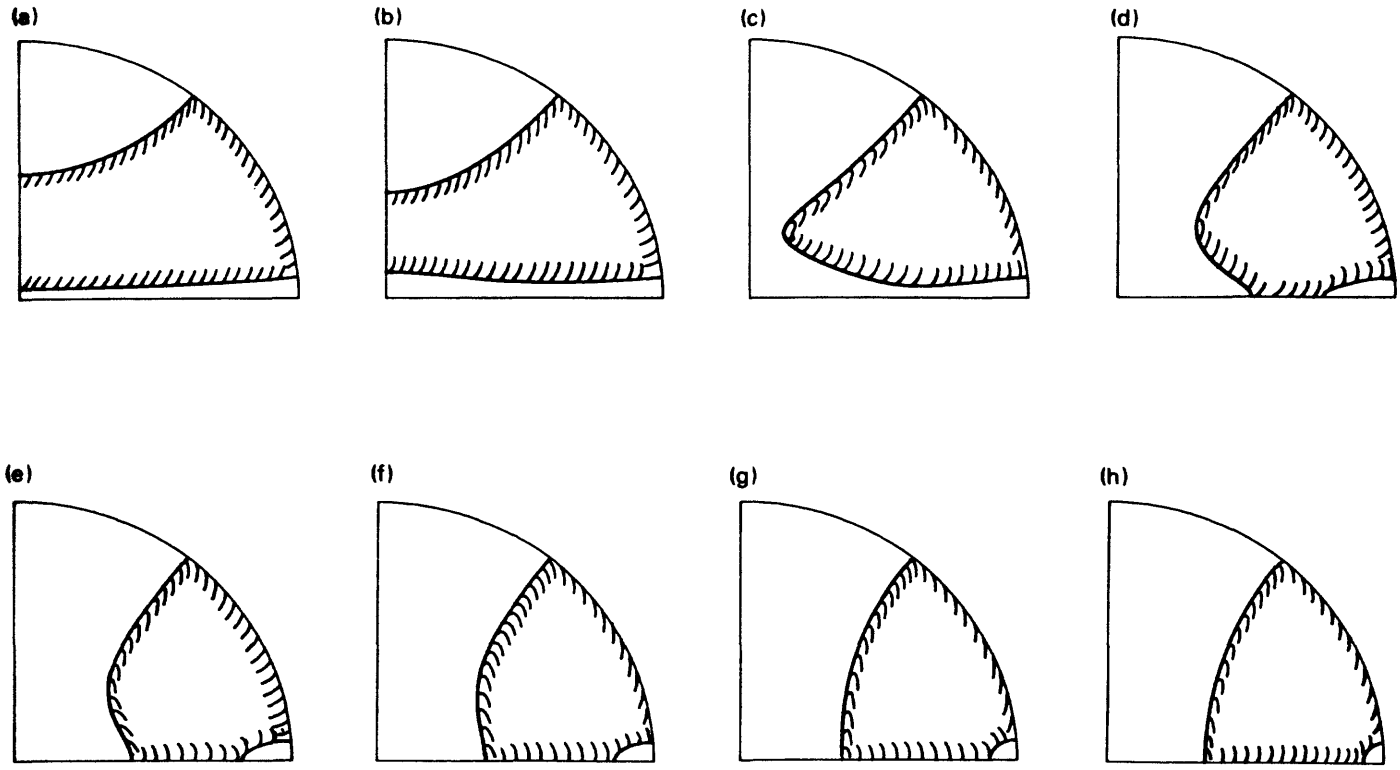

Fig. 2. Regions (shaded) in which the normal to a fault plane must fall for slip to occur. Three-dimensional loading $\sigma_z \geq \sigma_y \geq \sigma_x > 0$. Figures are for $\tan\phi_j = 0.67$, $\sigma_1 = 10\sigma_3$ and $\sigma_2/\sigma_3 = 1, 2, 3, 4, 5, 6, 8$, and 10 in (a)$\cdots$(h), respectively.

m equal to 2, 3, 4, 5, 6, and 8 for which σ_2 is intermediate between σ_1 and σ_3 are shown in Figures 2b-2g.

This example shows the influence of the intermediate principal stress on the range of fault orientations for which slip can take place. The possibility of strike-slip and oblique-slip motions on preexisting faults predominates throughout, whereas the pattern of low-angle reverse slip changes to dip slip with increase in σ_2. The extreme ratio of stresses, $\sigma_1 = 10\sigma_3$ ($n = 10$), used to generate these patterns of fault reactivation may be obtained in the shallow crustal environment under special conditions such as waterflooding. Reporting on an experiment in earthquake control at Rangely, Colorado, Raleigh et al. (1976) show that reservoir pressures during injection reached high values of about 28 MPa. This translates to an effective stress ratio of $n = 9.1$. The predicted pattern of fault slip corresponds with the observed distribution of focal plane solutions (Swolfs and Savage, 1987).

Figure 3 shows an example of slip and stable regions when one or two of the applied stresses are tensile. The friction angle Φ_j is equal to 30°. Assume first that σ_x and σ_z are positive with $\sigma_z = 0.1\sigma_x$ ($n = 0.1$). The stress σ_y is tensile with $\sigma_y = -0.8\sigma_x$ ($m = -0.8$). The extent of the stable and slip regions is limited to the domain of the reference circle for which $F_n = \sigma_n > 0$. This domain is located on the right hand side of the dashed line in Figure 3 corresponding to the condition $F_n = 0$. If both σ_x and σ_z are tensile, σ_y becomes compressive and the domain $F_n > 0$ is now located on the left hand side of the dashed line $F_n = 0$. This example shows that despite tensile loading in one or two directions, there are still stable and slip regions for which the normal stress across the faults remains compressive.

SUMMARY

The exact solutions presented in this paper provide a tool to better understand fault slip response to three dimensional crustal loading. The solutions presented here can be used to construct the domains in which the normal to a fault plane must fall for slip or stability to be possible and for which the fault normal stress always remains compressive. This can be done for a wide variety of loading conditions that can be found in shallow crustal environments with one or several stress components being tensile. The solutions also allow fault cohesion and pore pressure to be accounted for when assessing the extent of the slip and stable regions.

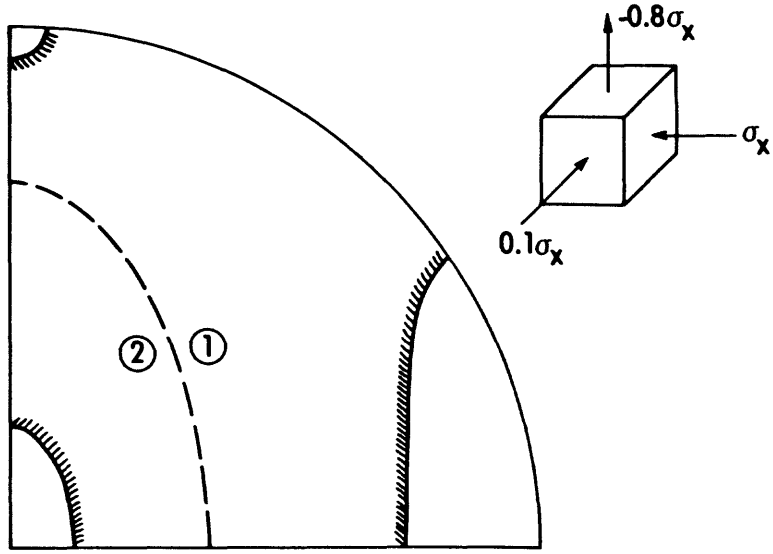

Fig. 3. Regions (shaded) in which the normal to a fault plane must fall for slip to take place. Three-dimensional state of stress σ_x, $\sigma_z = 0.1\sigma_x$ and $\sigma_y = -0.8\sigma_x$. The condition $F_n = 0$ is shown as a dashed line. Domain 1 is acceptable ($\sigma_n > 0$) when σ_x is positive. Domain 2 is acceptable ($\sigma_n > 0$) when σ_x is negative.

REFERENCES

1. Amadei, B., Robison, M.J., and Yassin, Y.Y., 1986, Rock Strength and the Design of Underground Excavations: Proceedings, International Symposium on Large Rock Caverns, Helsinki, Finland, __ p.

2. Beyer, W.H., 1985, CRC Standard Mathematical Tables: CRC Press, Inc., 27th ed., p. 9-12.

3. Bray, J.W., 1967, A Study of Jointed and Fractured Rock, Part I: Fracture Patterns and their Failure Characteristics: Rock Mechanics and Engineering Geology, p. 2-3, 117-136.

4. Brown, E.T., 1970, Strength and Models of Rock with Intermittent Joints: Journal of Soil Mechanics and Foundations, Division ASCE, 96, p. 1917-1934.

5. Einstein, H.H., and Hirschfeld, R.C., 1973, Model Studies on Mechanics of Jointed Rock: Journal of Soil Mechanics and Foundations, Division ASCE, 99, p. 229-248.

6. Goodman, R.E., and Shi, G.H., 1985, Block Theory and Its Application to Rock Engineering: New York, Prentice-Hall, 338 p.

7. Jaeger, J.C., 1960, Shear Failure of Anisotropic Rocks: Geology, 97, p. 65-78.

8. Jaeger, J.C., and Cook, N.G.W., 1976, Fundamentals of Rock Mechanics: New York, Chapman and Hall, p. 70-73.

9. Ladanyi, B., and Archambault, G., 1972, Evaluation de la Resistance au Cisaillement d'un Massif Rocheux Fragemente (in French): Proceedings, 24th International Geology Congress, 13D, p. 249-260.

10. Raleigh, C.B., Healy, J.H., and Bredehoeft, J.D., 1978, An Experiment in Earthquake Control at Rangely, Colorado: Science, 191, p. 1230-1237.

11. Reik, G., and Zacas, M., 1978, Strength and Deformation Characteristics of Jointed Media in True Triaxial Compression: International Journal of Rock Mechanics and Mineralogical Sciencei, 15, p. 295-303.

12. Savage, W.Z., and Swolfs, H.S., 1986, Tectonic and gravitational stresses in long symmetric ridges and valleys: Journal of Geophysical Research, 91, p. 3677-3685.

13. Savage, W.Z., and Swolfs, H.S., 1987, Slip--a Fortran Program for Computing the Potential for Sliding on Arbitrarily Oriented Weakness Planes in Triaxial Stress States: U.S. Geological Survey Open-File Report 87-82, 18 p.

14. Savage, W.Z., Swolfs, H.S., and Powers, P.S., 1985, Gravitational Stresses in Long Symmetric Ridges and Valleys: International Journal of Rock Mechanics and Mineralogical Science, 22, p. 291-302,

15. Swolfs, H.S., and Savage, W.Z., 1987, Analysis of slip potential in faulted rocks: Geological Society of America, Abstracts with Programs, 19, p. 338.

APPENDIX

```
C
C     AUTOMATIC GENERATION OF STEREO PLOTTING DATA FOR PREDICTION
C     OF FAULT SLIP UNDER MULTIAXIAL LOADING CONDITIONS.
C
      PROGRAM STEREO4
      REAL M,N,M1,MN
C
C     CRT SCREEN IS UNIT 6, KEYBOARD IS UNIT 5, OR *.
C
      WRITE(6,40)
C
C     READ IN ANGLE OF INTERNAL FRICTION (PHIA),
C     RADIUS OF STEREO NET (R), OUTPUT INCREMENT (XZBINC),
C     STRESS RATIO (M), AND STRESS RATIO (N).
C
      READ *, PHIA,R,XZBINC,M,N
      WRITE(6,50) PHIA,R,M,N
      WRITE(6,45)
C
C     INITIALIZE CONSTANTS
C
      PHI=PHIA*ATAN(1.)*4./180.
      CS2=1./(COS(PHI)**2)
      MN=M-N
      M1=M-1.
      A=-CS2*MN*MN
      B1=MN*(2.*M*CS2-M-N)
      B2=-2.*CS2*MN*M1
      C1=-CS2*M1*M1
      C2=M1*(2.*M*CS2-1.-M)
      C3=-M*M*(CS2-1.)
      SMINC=0.1*XZBINC
      WRITE(6,60)
      IF(M.EQ.N) GOTO 27
      XB=0.
C
C    * * * * * LOOP STRUCTURE * * * * *
C
  2   CONTINUE
      B=B1+B2*XB*XB
      C=(XB**4)*C1+XB*XB*C2+C3
      DELTA=B*B-4.*A*C
      IF(DELTA.LT.0.) GOTO 3
      D1=(-B+SQRT(DELTA))*0.5/A
      IF(D1.LT.0.) GOTO 3
      ZB1=SQRT(D1)
      DYB1=1.-XB*XB-ZB1*ZB1
      IF(DYB1.LT.0.) GOTO 3
```

```
      YB1=SQRT(DYB1)
      XO1=R*XB/(1.+YB1)
      ZO1=R*ZB1/(1.+YB1)
      WRITE(1,10) XO1,ZO1
      DIF1=1.-DYB1
      IF(DIF1.LT.0.9) THEN
          IF((XB.LE.0.1).OR.(ZB1.LE.0.1)) THEN
              XB=XB+SMINC
          ELSE
              XB=XB+XZBINC
          END IF
      ELSE
          XB=XB+SMINC
      END IF
      IF(XB.LE.1.) GOTO 2
    3 CONTINUE
      IF(XB.LE.0.1) THEN
          XB=XB+SMINC
      ELSE
          XB=XB+XZBINC
      END IF
      IF(XB.LE.1.) GOTO 2
C
C     * * * * * LOOP STRUCTURE * * * * *
C
      XB=0.
   20 CONTINUE
      B=B1+B2*XB*XB
      C=(XB**4)*C1+XB*XB*C2+C3
      DELTA=B*B-4.*A*C
      IF(DELTA.LT.0.) GOTO 24
      D2=(-B-SQRT(DELTA))*0.5/A
      IF(D2.LT.0.) GOTO 24
      ZB2=SQRT(D2)
      DYB2=1.-XB*XB-ZB2*ZB2
      IF(DYB2.LT.0.) GOTO 24
      YB2=SQRT(DYB2)
      XO2=R*XB/(1.+YB2)
      ZO2=R*ZB2/(1.+YB2)
      WRITE(1,10) XO2,ZO2
      DIF2=1.-DYB2
      IF(DIF2.LT.0.9) THEN
         IF((XB.LE.0.1).OR.(ZB2.LE.0.1)) THEN
             XB=XB+SMINC
         ELSE
             XB=XB+XZBINC
         END IF
      ELSE
         XB=XB+SMINC
      END IF
```

```
      IF(XB.LE.1.) GOTO 20
 24   CONTINUE
      IF(XB.LE.0.1) THEN
          XB=XB+SMINC
      ELSE
          XB=XB+XZBINC
      END IF
      IF(XB.LE.1.) GOTO 20
      GOTO 8
 27   CONTINUE
      DELTA=C2*C2-4.*C1*C3
      IF(DELTA.LT.0.) GOTO 36
      D1=(-C2+SQRT(DELTA))*0.5/C1
      IF(D1.LT.0.) GOTO 32
      XB1=SQRT(D1)
      IF(XB1.GT.1.) GOTO 32
      ZB=0.
C
C     * * * * * LOOP STRUCTURE * * * * *
C
 30   CONTINUE
      YB1=SQRT(1.-XB1*XB1-ZB*ZB)
      XO1=R*XB1/(1.+YB1)
      ZO1=R*ZB/(1.+YB1)
      WRITE(1,10) XO1,ZO1
      DIF1=XB1*XB1+ZB*ZB
      IF(DIF1.LT.0.9) THEN
         IF((ZB.LE.0.1).OR.(XB1.LE.0.1)) THEN
             ZB=ZB+SMINC
         ELSE
             ZB=ZB+XZBINC
         END IF
      ELSE
         ZB=ZB+SMINC
      END IF
      CHECK=XB1*XB1+ZB*ZB
      IF(CHECK.LE.1.) GOTO 30
 32   CONTINUE
      D2=(-C2-SQRT(DELTA))*0.5/C1
      IF(D2.LT.0.) GOTO 36
      XB2=SQRT(D2)
      IF(XB2.GT.1.) GOTO 36
      ZB=0.
```

```
C
C       * * * * * LOOP STRUCTURE * * * * *
C
 35     CONTINUE
        YB2=SQRT(1.-XB2*XB2-ZB*ZB)
        XO2=R*XB2/(1.+YB2)
        ZO2=R*ZB/(1.+YB2)
        WRITE(1,10) XO2,ZO2
        DIF2=XB2*XB2+ZB*ZB
        IF(DIF2.LT.0.9) THEN
           IF((ZB.LE.0.1).OR.(XB2.LE.0.1)) THEN
              ZB=ZB+SMINC
           ELSE
              ZB=ZB+XZBINC
           END IF
        ELSE
           ZB=ZB+SMINC
        END IF
        CHECK=XB2*XB2+ZB*ZB
        IF(CHECK.LE.1.) GOTO 35
 36     CONTINUE
        WRITE(6,80)
        IF(M.EQ.N) GOTO 49
        XB=0.
C
C       * * * * * LOOP STRUCTURE * * * * *
C
 40     CONTINUE
        D3=(M-XB*XB*M1)/MN
        IF (D3.LT.0.) GOTO 45
        ZB3=SQRT(D3)
        DYB3=1.-XB*XB-ZB3*ZB3
        IF(DYB3.LT.0.) GOTO 45
        YB3=SQRT(DYB3)
        XO3=R*XB/(1.+YB3)
        ZO3=R*ZB3/(1.+YB3)
        WRITE(2,10) XO3,ZO3
        DIF3=1.-DYB3
        IF(DIF3.LT.0.9) THEN
             IF ((XB.LE.0.1).OR.(ZB3.LE.0.1)) THEN
                XB=XB+SMINC
             ELSE
                XB=XB+XZBINC
             END IF
        ELSE
             XB=XB+SMINC
        END IF
        IF(XB.LE.1.) GOTO 40
 45     CONTINUE
```

```
      IF(XB.LE.0.1) THEN
         XB=XB+SMINC
      ELSE
         XB=XB+XZBINC
      END IF
      IF(XB.LE.1.) GOTO 40
      GOTO 100
   49 CONTINUE
      D3=M/M1
      IF(D3.LT.0.) GOTO 100
      XB3=SQRT(D3)
      IF(XB3.GT.1.) GOTO 100
      ZB=0.
C
C     * * * * * LAST LOOP * * * * *
C
   51 CONTINUE
      YB3=SQRT(1.-XB3*XB3-ZB*ZB)
      XO3=R*XB3/(1.+YB3)
      ZO3=R*ZB/(1.+YB3)
      WRITE(2,10) XO3,ZO3
      DIF3=XB3*XB3+ZB*ZB
      IF(DIF3.LT.0.9) THEN
         IF((ZB.LE.0.1).OR.(XB3.LE.0.1)) THEN
            ZB=ZB+SMINC
         ELSE
            ZB=ZB+XZBINC
         END IF
      ELSE
         ZB=ZB+SMINC
      END IF
      CHECK=XB3*XB3+ZB*ZB
      IF(CHECK.LE.1.) GOTO 51
  100 CONTINUE
C
C     * * * * FORMAT STATEMENTS * * * *
C
   10 FORMAT(2X,F10.4,2X,F10.4)
   40 FORMAT(10X,' ENTER PHI,R,XZBINC,M,N ')
   45 FORMAT(10X,' OUTPUT IS TO FILE FOR001.DAT')
   50 FORMAT(/10X,' FRICTION ANGLE ',F10.4/
     +        10X,' STEREO RADIUS  ',F10.4/
     +        10X,' SIGY:SIGX      ',F10.4/
     +        10X,' SIGZ:SIGX      ',F10.4//)
   60 FORMAT(/10X,' FAILURE CRITERION '//)
   80 FORMAT(/10X,' POSITIVE NORMAL STRESS CONDITION ')
      STOP
      END
```

Sample input for PHIA, R, XZBINC, M, N

30, 10, .1, 10, 1

Sample data output (FOR001.DAT)

XO	ZO
0.0000	3.0416
0.0546	3.0411
0.1093	3.0396
0.1639	3.0371
0.2185	3.0337
0.2731	3.0293
0.3278	3.0239
0.3824	3.0174
0.4370	3.0100
0.4916	3.0016
0.5463	2.9921
0.6009	2.9816
1.1471	2.8169
1.6934	2.5266
2.2396	2.0579
2.7859	1.2206
0.0000	9.3521
0.0937	9.3517
0.1875	9.3503
0.2812	9.3479
0.3749	9.3446
0.4687	9.3404
0.5624	9.3352
0.6561	9.3291
0.7498	9.3220
0.8436	9.3140
0.9373	9.3050
1.0310	9.2951
1.1248	9.2843
1.2185	9.2724
1.3122	9.2596
1.4060	9.2458
1.4997	9.2311
1.5934	9.2154
1.6872	9.1987
1.7809	9.1810

1.8746	9.1623
1.9684	9.1426
2.0621	9.1220
2.1558	9.1003
2.2495	9.0775
2.3433	9.0538
2.4370	9.0290
2.5307	9.0032
2.6245	8.9763
2.7182	8.9484
2.8119	8.9194
2.9057	8.8893
2.9994	8.8581
3.0931	8.8258
3.1869	8.7924
3.2806	8.7579
3.3743	8.7222
3.4681	8.6853
3.5618	8.6473
3.6555	8.6081
3.7492	8.5677
3.8430	8.5261
3.9367	8.4832
4.0304	8.4391
4.1242	8.3937
4.2179	8.3470
4.3116	8.2989
4.4054	8.2496
4.4991	8.1988
4.5928	8.1467
4.6866	8.0931
4.7803	8.0381
4.8740	7.9816
4.9677	7.9236
5.0615	7.8641
5.1552	7.8030
5.2489	7.7402
5.3427	7.6758
5.4364	7.6097
5.5301	7.5419
5.6239	7.4722
5.7176	7.4008
5.8113	7.3274
5.9051	7.2521
5.9988	7.1747
6.0925	7.0953
6.1863	7.0137
6.2800	6.9299
6.3737	6.8438

6.4675	6.7553
6.5612	6.6643
6.6549	6.5707
6.7486	6.4744
6.8424	6.3753
6.9361	6.2732
7.0298	6.1680
7.1236	6.0595
7.2173	5.9475
7.3110	5.8319
7.4048	5.7124
7.4985	5.5888
7.5922	5.4608
7.6860	5.3281
7.7797	5.1903
7.8734	5.0469
7.9671	4.8976
8.0609	4.7418
8.1546	4.5787
8.2483	4.4076
8.3421	4.2276
8.4358	4.0373
8.5295	3.8353
8.6233	3.6196
8.7170	3.3877
8.8107	3.1358
8.9045	2.8588
8.9982	2.5485
9.0919	2.1907
9.1856	1.7568
9.2794	1.1642